

Article

Improving of Mechanical Properties of Titanium Alloy VT23 due to Impact-Oscillatory Loading and the Use of Carbon Nano-Solution

Mykola Chausov ¹, Oleg Khyzhun ², Janette Brezinová ^{3,*}, Pavlo Maruschak ⁴ , Andrii Pylypenko ¹, Jozef Brezina ⁵, Katarína Buzová ⁵ and Kostiantyn Lopat'ko ¹

- ¹ Department of Mechanics, National University of Life and Environmental Sciences of Ukraine, HeroivOborony str.15, 03041 Kyiv, Ukraine; m.g.chausov@gmail.com (M.C.); andriy3pl@gmail.com (A.P.); lopatko_konst@hotmail.com (K.L.)
- ² Institute for Problems of Materials Science National Academy of Sciences of Ukraine, Krzhizhanovsky str.3, Ukraine, 03142 Kyiv, Ukraine; khyzhun@ipms.kiev.ua
- ³ Department of Engineering Technologies and Materials, Faculty of Mechanical Engineering, Technical University of Košice, Mäsiarska 74, 040 01 Košice, Slovakia
- ⁴ Department of Industrial Automation, Ternopil National Ivan Puľuj Technical University, Ruska str. 56, 46001 Ternopil, Ukraine; maruschak.tu.edu@gmail.com
- ⁵ 1st Surgical Clinic of Faculty of Medicine PavolJozefŠafárik University in Košice and University Hospital of L. Pasteur in Košice, 04022 Košice, Slovakia; brezinamudr@gmail.com (J.B.); katarina.katka87@gmail.com (K.B.)
- * Correspondence: janette.brezinova@tuke.sk; Tel.: +421-55-602-3542

Received: 9 May 2019; Accepted: 3 June 2019; Published: 4 June 2019



Abstract: Improvement in the mechanical properties of sheet two-phase high-strength titanium alloy VT23 due to impact-oscillatory loading and the use of carbon nanosolutions at room temperature was tested experimentally. It was shown that in addition to obtaining a significant increase in the initial plastic deformation of the alloy, it is possible to strengthen the surface layers of the alloy by a factor of 8.4% at a time via the impulse introduction of energy into the alloy and the use of carbon nanosolutions. Using X-ray photoelectron spectroscopy (XPS), it was first found that strengthening of the surface layers of the titanium alloy at a given load, in line with using a carbon nanosolution, leads to the formation of a mixture of titanium oxide and titanium carbide or oxycarbide of type $TiO_{2-x}C_x$ on the surface.

Keywords: impact-oscillatory loading; nanotechnology; titanium alloy; surface layers; strengthening; titanium carbide

1. Introduction

Fundamental research on high-strength titanium alloys and their use in the military, aviation, and space industries have proven their high-performance properties [1–5]. The most common titanium alloys are those representing α and β solid solutions. Alloys with an ($\alpha + \beta$) structure provide optimal characteristics of strength, ductility, and crack resistance and extend the life of machine parts [6–8].

At the same time, there is a certain tendency to a reduction in the plasticity and crack resistance of alloys and an increase in their sensitivity to stress concentrators as the strength of such alloys increases. That is why methods for modifying their properties which make it possible to preserve the high strength of these alloys while increasing their plasticity are very relevant [9–11].

Fundamental regularities in the mechanical behavior of structural materials under dynamic non-balanced processes, which are associated with high-speed energy exchange between the elements of mechanical systems, have not been sufficiently studied to date [12–15]. The difficulties of applied

research are associated, first of all, with the lack of experimental facilities and equipment for such mechanical tests.

We propose an effective method for reproducing dynamic non-equilibrium processes (DNP) using impact-oscillatory loading under high-speed stretching of a material with the imposition of a high frequency (several kilohertz) oscillatory process [16–18]. As a result of the conducted research, a number of specific features of material deformation during and after the realization of DNP were found; these are manifested, first of all, in the plasticization of materials of different classes under subsequent static tensile testing due to the formation of dissipative microstrip structures, interconnected at different scale levels, the density of which is much lower than that of the source material [19–21].

Sudden increases in deformation under impulse introduction of energy ε_{imp} were chosen as a parameter characterizing the intensity of the impulse introduction of energy into materials. The choice of ε_{imp} significantly simplifies the test procedure under impact-oscillatory loading. In this case, modes of impact-oscillatory loading can be created on hydraulic machines of varying rigidity, eliminating the need for complex calculations on the transfer of a particular force influence directly on a specimen, depending on the total pulse applied to the mechanical system. In addition, such a procedure is intended specifically for real technological processes and can be realized in industrial conditions.

Using Phantom v711 a high-speed camera (the maximum recording speed is 1,400,000 f/s), two stages of the low- and high-speed process, which are responsible for the formation and development of a dissipative structure in materials under impact-oscillatory loading, were found. The mean deformation rates in the first stage of the process were 100–300%/s for aluminum alloy D16 and aluminum alloy 2024-T3 [19], and 100–200%/s for stainless steel 12Cr17 [20]. At the second stage, where the newly formed dissipative structure probably propagates through the volume of the specimen under study, a sharp increase in the deformation rate up to 5000–6000%/s was observed in local zones for aluminum alloys D16 and 2024-T3 [19] and up to 600–1000%/s for stainless steel 12Cr17 [20]. It was also established that the frequency of oscillatory loading which is realized under impact-oscillatory loading of materials is in the range of 1–2 kHz [19,21].

An explicit consequence of the significant structural transformations of materials under impact-oscillatory loading is the appearance of microextrusions on the specimen surface due to the formation of less dense dissipative structures [22]. This effect indicates changes in the structure and mechanical properties not only in the volume of materials, but, above all, in the surface layers. In addition, a special plastic “wave” which passed along the surface of flat specimens during the realization of DNP [20] was found. The front of this “wave” moves at a low speed. For instance, for stainless steel 12Cr17, this speed is 0.3–0.7 m/s. However, the fact of the appearance of the plastic “wave” under impact-oscillatory loading and the appearance of microextrusions on the specimen surface allow us to assume that it is possible to realize very high stresses at local points of the surface layers of materials.

When DNP is realized in materials of other classes, one should expect the formation of new forms of dissipative structures. For example, when DNP is realized in two-phase high-strength titanium alloy VT22, a change in the initial structure occurs by grinding (fragmentation) of the β -phase and subgrains in this phase [23]. Detailed investigations of the metal–physical aspects of the structure of the VT22 alloy before and after impact-oscillatory loading revealed the peculiarities in the formation of less dense dissipative structures in two-phase titanium alloys [23].

We used the discovered effects to develop an effective method for strengthening and nanostructuring the surface of materials and obtaining a uniform, controlled nanostructure of the surface layer with enhanced mechanical strength via impact-oscillatory loading and nanotechnologies [24]. The technology of this method is as follows. Prior to impulse loading, specimen surfaces are wetted with a colloidal solution of nanoparticles (metals or hard alloys, carbides or nitrides), and nanoparticles are precipitated from the solution onto the surface of materials by means of drying. As a result of pre-wetting with a given colloidal solution under the dynamic non-balanced process, hard alloy nanoparticles located on the surface of the test material are “embossed” into the surface due to the

occurrence of microextrusions, which leads to significant structural changes in the surface layer with the formation of a controlled nanostructured surface layer. The controlled structure of the material surface is obtained by adding hard alloy nanoparticles of appropriate size to the colloidal solution and using a solution of the relevant concentration.

The purpose of this study was to further modify of the mechanical properties of two-phase titanium alloys by simultaneously using impact-oscillatory loading and carbon nanosolution and to analyze the physical aspects of the detected mechanical effects.

2. Materials and Methods

We used combined loading which included the application of additional force pulses to the base loading. This is a follow-up on our previous research aimed at a significant increase in material plasticity at room temperature. In this case, the processes of material deformation and fracture are studied within a mechanical system that includes two contours. The internal contour is a simple statically indeterminate structure in the form of three parallel elements loaded simultaneously: the central specimen from the test material and two symmetrical satellite specimens from brittle steel. The external contour includes the gripping of the test setup, columns, and the hydraulic system of the test setup. With the controlled fracture of the satellite specimens of the internal contour, the pulsed load is transmitted to the external contour of the test setup, and the test specimen, together with the external contour of the test setup is subjected to additional load pulses applied to the base loading (impact-oscillatory loading) at a frequency of 1–2 kHz [17–19].

Mechanical tests were performed on specimens of sheet two-phase high-strength alloy VT23 with a thickness of 3 mm (Figure 1). The ZD-100Pu (WPM, Leipzig, Germany) modified hydraulic setup for static tests were used.

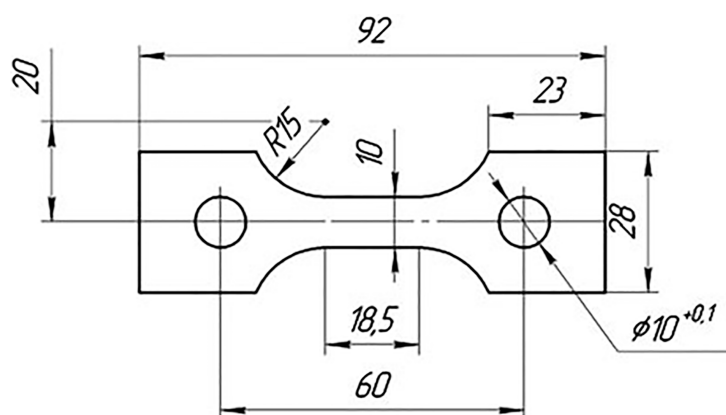


Figure 1. Test specimen.

To obtain a carbon nanosolution, an aqueous dispersion of carbon, and the possibility of extending the physical and chemical activity of its particles, the method of electroerosive dispersion of graphite granules in water was used [25]. Using a thyristor generator (NULES, Kyiv, Ukraine) with a capacitive energy storage device, we formed discharge pulses, the voltage amplitude of which was regulated within the range of 90 V and the current in the range of 1000 A. The capacity C of the energy storage device was regulated in the range of 200 μF and the frequency of the discharge pulses was regulated in the range of 200 Hz, while pulse duration was 100 μs . The inductance of the discharge loop L did not exceed 1 μH .

Deionized water, characterized by a conductivity of $\sim 1 \times 10^{-6} - 3 \times 10^{-6} \text{ Ohm}^{-1}/\text{cm}$, is a convenient object for obtaining aqueous carbon dispersions. Water is used not only as a dispersion medium but also as a component of micelles, which are an active participant in the structure formation process and the process of formation of the electrokinetic potential of dispersions. At the same time, for each

type of dispersion, there are optimal time and temperature modes for the formation of micelles, at which a high concentration of the disperse phase is achieved and particles of minimal size are formed. Aqueous dispersions of metals and carbon are classified as lyophobic systems, the dispersed phase of which is water-wetted to a limited extent. They have input surface energy and thermodynamic instability. When the aqueous dispersion is stored for a long time, its fracture gradually occurs due to a drop in the ζ potential and the attainment of its threshold or critical value. The resulting aqueous dispersions of carbon are characterized by a high concentration of dispersed phase (1000 mg/md³) with average dimensions in the cross section of not more than 10 nm. The morphology of the resulting tubular carbon structures does not correspond to the classical concepts of nanotubes and is more like a “nanoplug”, the length of which is commensurable with the transverse dimensions of synthesized nanostructured objects. Single-walled nanotubes were used, which differed in the concentration of the dispersed phase of carbon due to the change in the time of impulse processing from 1 to 3 min. Carbon nanosolution of three concentrations were applied directly to the original surface of nine specimens under study, but the surfaces of three specimens were polished prior to the application of the colloidal solution with maximal concentration.

The polishing procedure itself was not decisive in this case; it was conducted only to evaluate the impact of surface roughness on the effect of strengthening the surface layers. To verify the occurrence of microextrusions on the specimen surface due to the formation of less dense dissipative structures under impact-oscillatory loading and to evaluate their effect on the initial surface roughness of specimens, a profilometric analysis of the topography of the alloy surface layers was performed using the Leica DCM8 3D optical surface metrology system (Leica Mikrosysteme Vertrieb GmbH, Wetzlar, Germany). The X-ray photoelectron spectroscopy (XPS) (SPECS Surface Nano Analysis Company, Berlin, Germany) method was used to investigate the surface layers of specimens of the VT23 alloy after the realization of impact-oscillatory loading. XPS-spectra were measured in a UHV Analysis System chamber at a residual pressure of less than 8×10^{-8} Pa. The XPS spectra were examined using an X-ray MgK α -radiation source ($E = 1253.6$ eV) and recorded at a constant retarding potential of 30 eV.

The chemical composition of the test alloy is given in Table 1.

Table 1. Chemical composition of VT23 titanium alloy (wt %).

Fe	Cr	Mo	V	Ti	Al
0.6	1.2	2.0	4.3	86.9	5.0

The microstructure of the VT23 alloy in its initial state is shown in Figure 2.

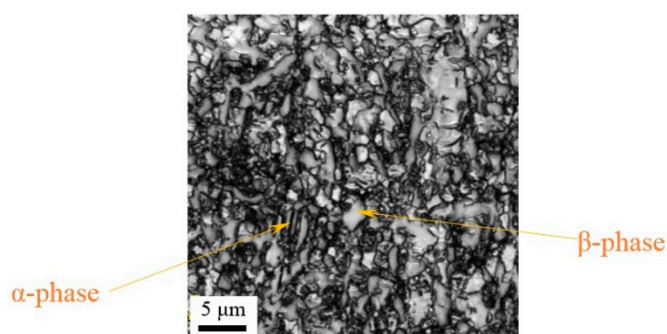


Figure 2. Microstructure of the VT23 alloy.

In a previous X-ray study, it was found that the β phase occupies 43.5% by weight and the α phase occupies 56.5% by weight in the investigated VT23 alloy. This method is described in detail in [26]. All investigations were conducted at 20 °C.

The research was conducted in two stages. In the first stage, the optimal effect of the intensity of the impulse introduction of energy under impact-oscillatory loading on the maximum increase in the initial plastic deformation of the VT23 alloy was revealed for a batch of specimens.

When evaluating the effect of impact-oscillatory loading on the improvement of the plastic properties of the titanium VT23 alloy, the following method of controlling the impulse introduction of energy into the titanium alloy was used; a number of specimens were statically loaded to a growing deformation level of 0.025–0.4%, and then the specimens were subjected to force impulse loading within a narrow range of 120 ± 5 kN.

In the second stage, with the selected optimal impact-oscillatory loadings ε_{imp} , a complex study was conducted on the impact-oscillatory loading and the use of carbon nanosolutions.

3. Results and Discussion

3.1. Results of Mechanical Tests

Analysis of the results obtained showed the following: if during the impulse introduction of energy into the VT23 titanium alloy the total stress from the previous static tensile testing and impulse introduction of energy does not exceed the yield strength of the alloy, the effect of increasing plastic deformation of the alloy under repeated static tensile testing is negligible. It should also be noted that the impulse introduction of energy in this case does not affect the strength properties of the alloy.

In the case when the VT23 alloy deforms plastically during the impulse introduction of energy, a marked increase in plastic deformation at repeated static tensile testing is observed in comparison with the initial state. Moreover, this dependence is complex and is associated with the degree of jumps of plastic deformation under the impulse introduction of energy ε_{imp} . For example, Figure 3 shows some data on the effect of impulse introduction of energy on the enhancement of plastic deformation of the VT23 alloy under repeated static tensile testing. As can be seen from Figure 3, the impulse introduction of energy in this case practically does not affect the strength properties of the alloy.

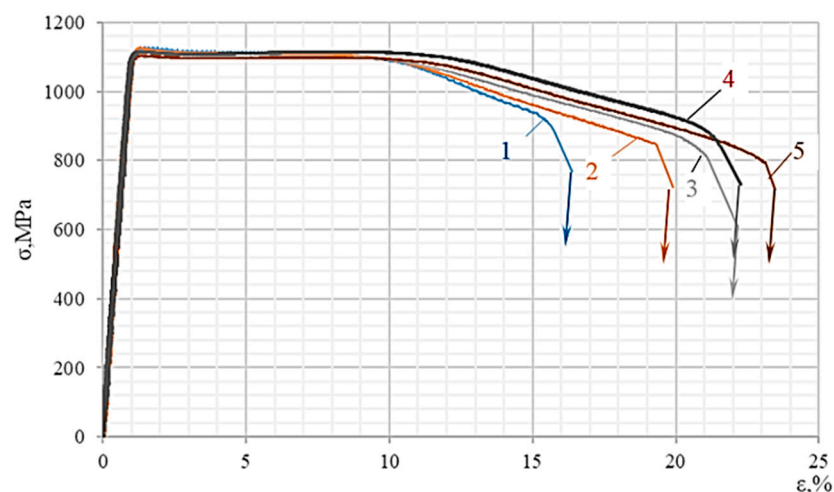


Figure 3. Typical stress strain diagrams for the VT23 alloy under static tensile testing after impulse introduction of energy under impact-oscillatory loading compared with the initial state: 1: initial state; 2: $\varepsilon_{imp} = 1.5\%$; 3, $\varepsilon_{imp} = 3.9\%$; 4: 3.8% ; 5: 3.65% .

It is interesting to note that along with the significant structural transformations in the volume of titanium alloys under DNP [23], which change the mechanical properties under subsequent deformation, similar effects caused by structural changes also arise on the specimen surface, even under insignificant influence from the impulse. For example, Figure 4 shows a comparison of the topographies of flat specimen surfaces of the VT23 alloy in the initial state and after the realization of low-density DNP ($\varepsilon_{imp} = 0.85\%$) using the Leica DCM8 3D optical surface metrology system. In all cases, the direction

of figure arrangement on the larger side coincides with the direction of deformation. For ease of comparison, the results obtained for the investigated alloy are presented and analyzed in pairs. Here, Figure 4a,c correspond to specimens in the initial state, and Figure 4b,d correspond to specimens after impact-oscillatory loading.

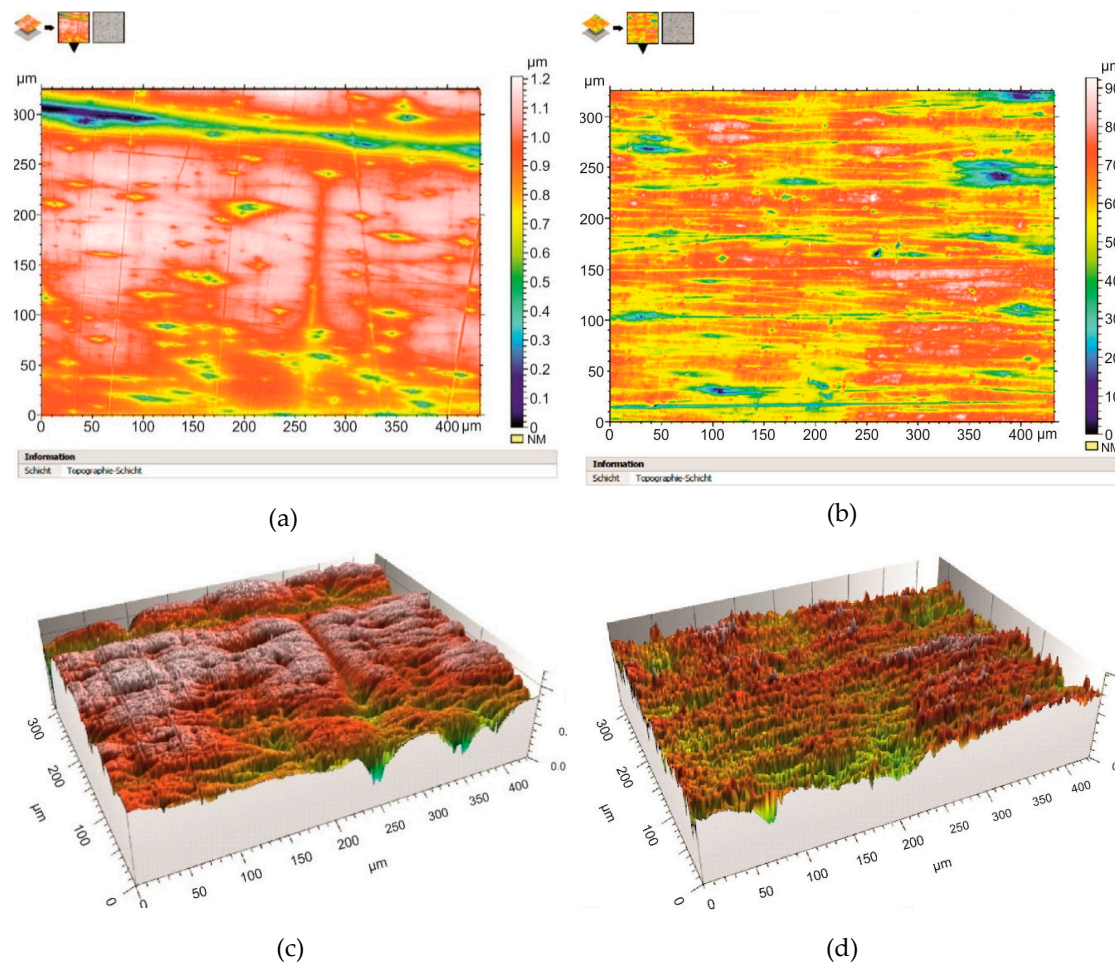


Figure 4. Topographies of plane surfaces of samples of the VT23 alloy in the initial state (a,c) and after DNP ($\varepsilon_{imp} = 0.85\%$) (b,d): (a,b), 2D measurements; (c,d), 3D measurements.

Let us note that the topographies of the flat surfaces of specimens under study were significantly different. The effect of impulse introduction of energy manifests itself clearly in the alignment of the specimen surface profile and in the creation of a regular ordered system of microextrusions on the surface. Moreover, after the realization of DNP, the surface structure becomes fibrous and oriented in the direction of loading.

The surface roughness parameters were determined according to the roughness standard DIN EN ISO 4287: 2010. Data were processed based on the “extraction” of a profile with a length of 300 μm in parallel with the load axis. In the measured topographic plot, three lines along which the profile was taken were drawn conventionally. The lines were located approximately evenly in the upper, middle, and lower part of the plot. The data processing results yielded the following values. In the initial state, Rz and Ra are 113, 202, and 101 μm and 15.1, 34.2, and 13.3 μm , respectively, and for the alloy after the DNP, they are 154, 112, and 154 μm and 18, 15.7, and 22, 8 μm , respectively.

Thus, an analysis of Figure 4 showed that even with insignificant intensity of the impulse introduction of energy into the alloy, there are changes in the topography of the surface with remarkable signs of surface alignment and the appearance of a regular ordered system of microextrusions. Naturally,

for each material there is its optimum intensity of the impulse introduction of energy which provides the maximum improvement in the mechanical properties of the material under subsequent loading.

Using the discovered effect, namely, the dependence of plastic deformation jumps under impulse introduction of energy on the plastic deformation of VT23 alloy under subsequent static tensile testing, we substantiated the optimal mode of impulse introduction of energy in order to maximize the plastic deformation of the VT23 alloy compared to its initial state. In particular, with $\varepsilon_{imp} = 3\text{--}4\%$, the plastic deformation of the titanium VT23 alloy can be increased by 35–40%.

The above optimal effect, i.e., using high-intensity impulse introduction of energy into the VT23 titanium alloy in order to increase the plastic deformation of the alloy, was taken into account in further experiments. For the second batch of specimens, the strengthening of surface layers of the alloy by a colloidal carbon solution was performed simultaneously with the impulse introduction of energy into the alloy. The colloidal solution was applied to the working part of the specimens. The strengthening of the surface layers of the VT23 alloy was assessed as follows. After the application of additional impulse loads, the specimens were completely unloaded and rubbed with alcohol; then, using an NPO-10 hardness tester, the hardness of the surface layer was measured by the Vickers method in the working area and, for comparison, at the specimen head with a working load of 10 kg. The number of indentations used for each study area of the surface was not less than 30. Figure 5 presents some experimental results.

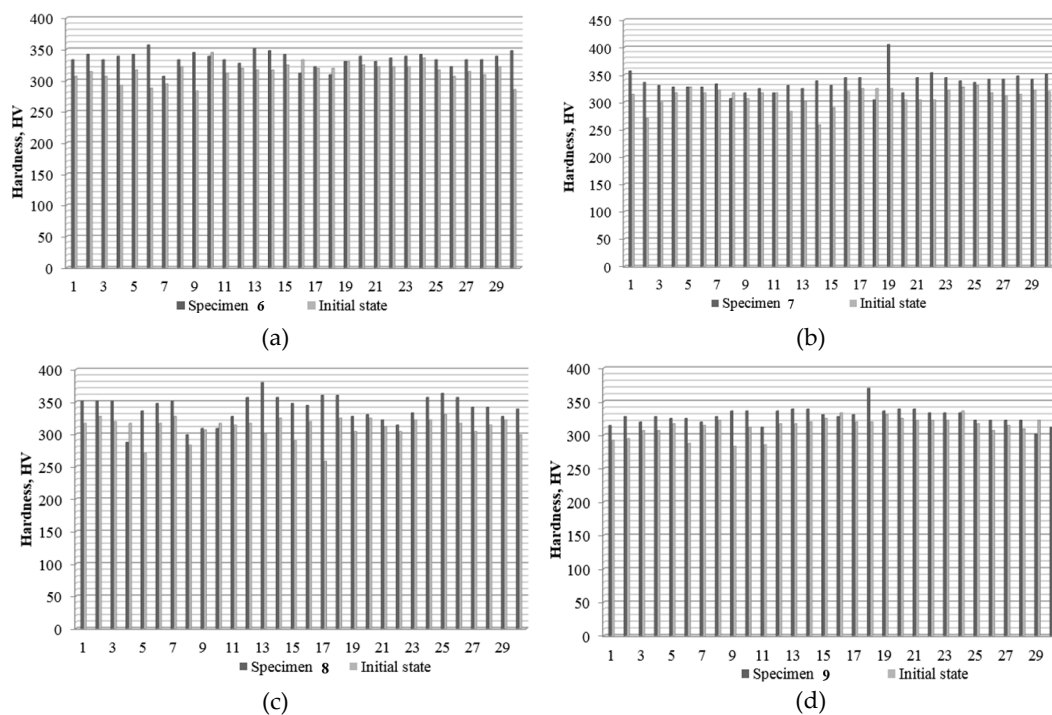


Figure 5. Increase in hardness compared to the initial state of the specimen surface layer of VT23 alloy treated with carbon nanosolutions of different concentration: (a–c) by 6.0%, 7.5%, and 8.4%, respectively; (d) polished surface by 4.4%.

Here, the values of hardness which are indicated by specimen 6, 7, 8, and 9 correspond to the hardness of the working part of the specimens with the deposited carbon nanosolution. The values of hardness which are indicated as the initial state correspond to the hardness of the gripping parts of the same specimens.

An analysis of the results obtained showed that by using carbon nanosolution of different concentrations, one can increase the macrohardness of the surface layers of the VT23 titanium alloy by an average of 6.0–8.4% (see Figure 5a–c). It is also possible to state unequivocally that the macrohardness of surface layers of the VT23 titanium alloy depends on the concentration of the carbon

nanosolution and the sizes of the nanoparticles. On the pre-polished specimens, the effect of increasing the microhardness of the surface layers is less pronounced up to 4.4% on average (see Figure 5d). This can be explained in the following way: it is easier for nanoparticles of the carbon nanosolution to be “embossed” into the surface layers of the alloy when there is initial roughness on the surface on which microextrusions are superimposed due to the formation of less dense dissipative structures in the alloy. In the process of conducting such tests, a natural question arises as to the homogeneity of the surface layer reinforced by this method. The results of the evaluation of the statistical characteristics of scatter of the measured hardness values in particular, the standard deviation and the variation factor are shown in Table 2.

Table 2. Statistical characteristics of scatter of the measured hardness values of the investigated specimens (see also Figure 5).

Specimens	Mean Hardness, HV		Standard Deviation, HV		Variation Factor, C, %	
	Working Surface	Initial State of the Specimen	Working Surface	Initial State of the Specimen	Working Surface	Initial State of the Specimen
6	334.38	314.04	11.36	14.47	3.4	4.6
7	336.01	310.75	18.12	16.6	5.4	5.3
8	339.72	310.75	20.48	16.6	5.3	6.0
9	328.34	314.04	11.93	14.47	3.6	4.6

Analysis of the data presented in Table 2 shows that for virtually all tested specimens, the surface layers of the working parts are not less homogenous in terms of hardness compared with the initial state of the alloy. In order to explain the detected effect of strengthening the surface layers of the investigated titanium alloy, detailed physical studies of one of the unpolished specimens were conducted using the X-ray photoelectron spectroscopy (XPS) method. In this case, a specimen with maximum strengthening of the surface layer (8.4%) was chosen.

3.2. Physical Results

As can be seen from Figure 6, titanium, oxygen, and carbon are present on the surface of the specimen under consideration after the realization of impact-oscillatory loading. Oxygen registered as both adsorbed and bound (as a result of the formation of Ti–O bonds) (Figure 7). The binding energy of Ti_{2p}-electrons corresponds to titanium in the charge state of Ti⁴⁺, probably due to the formation of titanium dioxide on the surface (Figure 8), while the binding energy of the C_{1s}-electrons (Figure 9) corresponds to the hydrocarbon adsorbed on the surface of the test specimen as a result of its prolonged exposure to air.

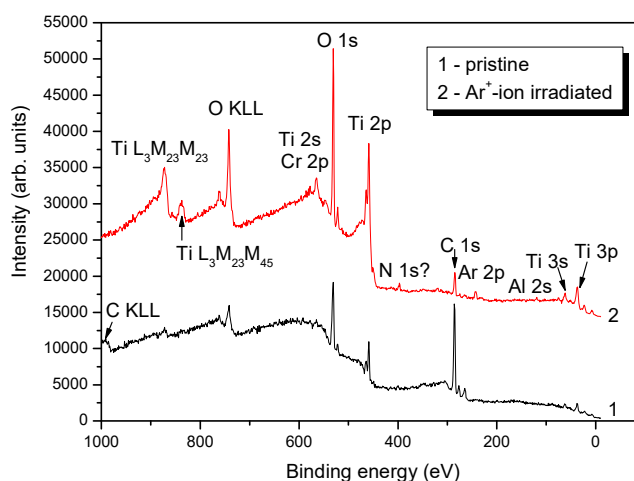


Figure 6. Panoramic XPS spectra of the investigated specimen before (1) and after (2) cleaning its surface with Ar⁺ ions.

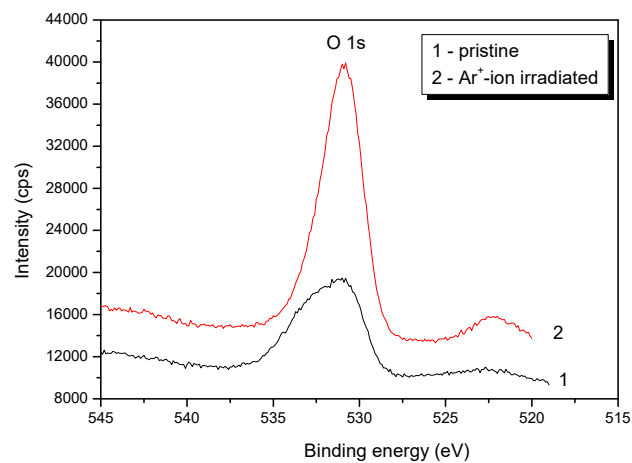


Figure 7. XPS spectra of the internal O_{1s}-electrons of the investigated specimen before (1) and after (2) cleaning its surface with Ar⁺ ions.

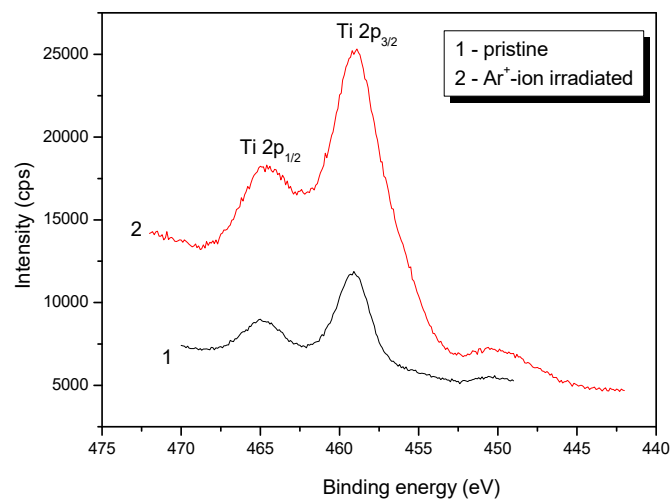


Figure 8. XPS spectra of internal Ti_{2p} electrons of the investigated specimen before (1) and after (2) cleaning its surface with Ar⁺ ions.

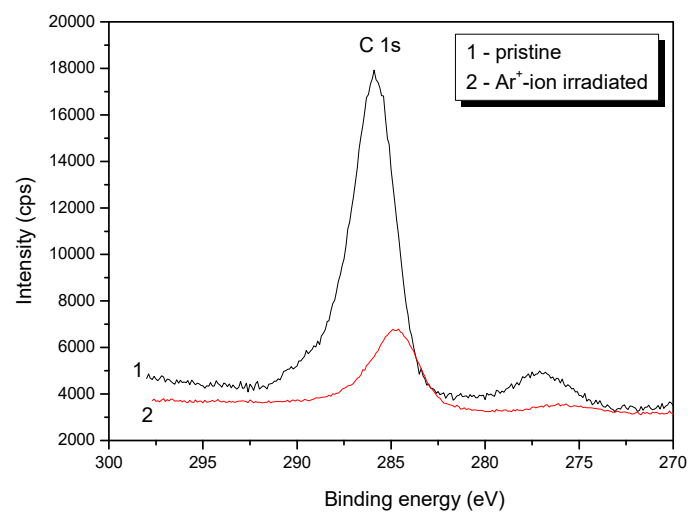


Figure 9. XPS spectra of the internal C_{1s}-electrons of the investigated specimen before (1) and after (2) cleaning its surface with Ar⁺ ions.

After cleaning with Ar^+ ions, no contributions from adsorbed hydrocarbons and oxygen were observed on the surface of the test specimen, particularly, on the spectra of the internal O_{1s} - and C_{1s} -electrons (Figures 7 and 9). The binding energy of the C_{1s} -electrons corresponds to that of graphite. On the surface of the test specimen, after its treatment with Ar^+ ions, only oxygen bound with titanium was observed as a result of the formation of a film of titanium dioxide upon prolonged exposure to air. However, cleaning with Ar^+ ions led to the rupture of some Ti-O bonds, and features of the $\text{Ti}2p$ electron spectrum corresponding to titanium in the metallic state of Ti^0 (in addition to $\text{Ti}_4 \text{Ti}^{4+}$) were then observed on the surface under study. The presence of titanium in the two charge states (Ti^0 and Ti^{4+}) on the surface under investigation was also confirmed by the results of investigation into the Auger lines $\text{TiL}_3\text{M}_{23}\text{M}_{23}$ and $\text{TiL}_3\text{M}_{23}\text{M}_{45}$ (Figure 10).

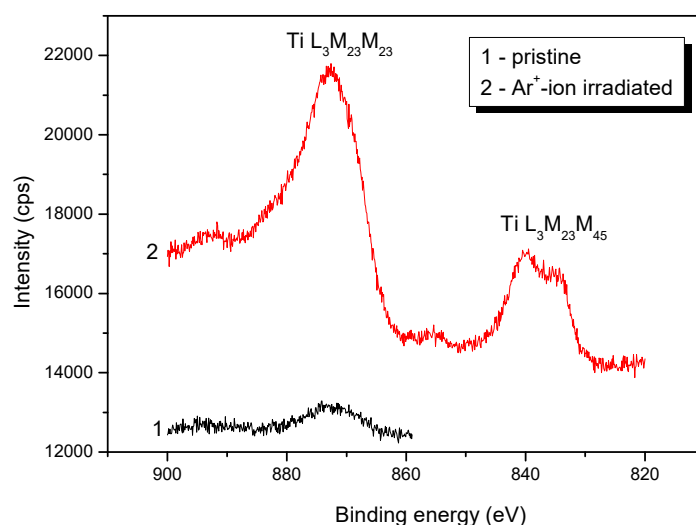


Figure 10. Auger lines $\text{TiL}_3\text{M}_{23}\text{M}_{23}$ and $\text{TiL}_3\text{M}_{23}\text{M}_{45}$ of the investigated specimen before (1) and after (2) cleaning its surface with Ar^+ ions.

Analysis of the energy position of the peaks of the C_{1s} spectra showed that prior to cleaning, the position of the $1s$ line corresponded to the pure carbon $EC_{1s} = 284.6$ eV, whereas after argon cleaning, this line shifted by 1.2 eV towards the lower binding energies, and its peak corresponded to energy $EC_{1s} = 285.8$ eV (Figure 9). This indicates the taking of electrons by carbon and the reduction of its positive charge. Since the electron affinity in carbon is greater than that in titanium and much lower than in oxygen, this electron transfer is possible only from titanium. Consequently, a transfer of this kind is possible only with the formation of Ti-C bonds. In addition, after cleaning, a shift occurred toward lower binding energies (Figure 8): the $\text{Ti}2p_{3/2}$ - and $\text{Ti}2p_{1/2}$ - lines shifted by 0.2 eV and 0.4 eV, respectively. This is due to the fact that carbon takes fewer electrons than oxygen. However, small shifts in the lines of titanium indicate that there were more Ti-O bonds than Ti-C bonds. Thus, after cleaning, there was a mixture of titanium oxide and titanium carbide or titanium oxycarbide such as $\text{TiO}_{2-x}\text{C}_x$ on the specimen surface. A mixture of titanium oxide and titanium carbide or titanium oxycarbide of the $\text{TiO}_{2-x}\text{C}_x$ type found on the specimen surface generally confirms our working hypothesis concerning the strengthening of the surface layers of the alloy via impact-oscillatory loading and the use of carbon nanosolutions. Indeed, less dense dissipative structures that are created in the volume of the alloy under impact-oscillatory loading are microextruded onto the surface of the specimen, and when the plastic “wave” passes, they are embossed into the alloy, resulting in significant structural changes in the surface layer with the formation of the surface nanostructured layer [27–31].

4. Conclusions

By way of tests involving sheet VT23 titanium alloy, the positive effect of impact-oscillatory loading on the improvement of the plastic deformation of this two-phase high-strength titanium alloy was

confirmed. It was shown that when the jumps of plastic deformation reach the values $\varepsilon_{imp} = 3.0\text{--}4.0\%$ in the process of impulse introduction of energy into the VT23 alloy, the plastic deformation of the alloy increases by 35.0–40.0% under repeated static tensile testing.

Using 3D optical surface measurement, it was found that even with a slight impulse effect on the VT23 alloy, the topography of the specimen surface layer changes significantly compared to the initial state. The main feature of such changes is the appearance of a regular ordered system of microextrusions on the specimen surface due to the formation of less dense dissipative structures in the alloy volume. The fact of the appearance of microextrusions on the specimen surface was used as the basis for the creation of a composite method for improving the mechanical properties of materials via impact-oscillatory loading and the use of nanotechnologies.

This method for improving the mechanical properties of titanium alloys was tested via the optimal impulse introduction of energy in to the VT23 alloy and the use of carbon nanosolutions. It was shown experimentally for the first time that via the impulse introduction of energy and the use of carbon nanosolution, one can significantly increase the initial plastic deformation of sheet high-strength two-phase VT23 titanium alloy by 35.0–40.0% and the macrohardness of its surface layers by a factor of 8.4% at a time.

X-ray photoelectron spectroscopy (XPS) was used to establish that the strengthening of the surface layers of VT23 titanium alloy due to impact-oscillatory loading and the use of the carbon nanosolution is associated with the formation of a mixture of titanium oxide and titanium carbide or titanium oxycarbide of the $\text{TiO}_{2-x}\text{C}_x$ type on the specimen surface.

Thus, the formation of a mixture of titanium oxide and titanium carbide or titanium oxycarbide of the $\text{TiO}_{2-x}\text{C}_x$ type due to impact-oscillatory loading and the use of carbon nanosolution at room temperature was recorded for the first time.

The basic regularities in the influence of nanosolutions and impact-oscillatory loading of different intensities on changes in the physical and mechanical properties of bulk and superficial layers of two-phase titanium alloys were established; this will contribute to the formulation of a physical–mechanical model of the influence of DNP caused by impact-oscillatory loading on the mechanical properties of titanium alloys. These scientific results may also have practical applications in the complex modification of titanium alloys in medicine and in the production of means of personal protection (such as body armor).

Author Contributions: Conceptualization, M.C.; Formal analysis, J.B. and P.M., O.K., K.L.; Investigation, M.C., J.B., A.P., P.M., O.K., K.L.; Methodology, M.C. and A.P.; Project administration, P.M.; Validation, P.M., M.C., A.P., J.B.; Writing—original draft, P.M., M.C., J.B., A.P.; Writing—review and editing, J.B., K.B.

Funding: This research was funded by Ministry of Education of the Slovak Republic VEGA No. 1/0424/17 and by the Slovak Research and Development Agency APVV-16-0359, and the APC was funded by the Slovak Research and Development Agency.

Acknowledgments: This work was supported by the scientific grant agency of the Ministry of Education of the Slovak Republic VEGA No. 1/0424/17 and by the Slovak Research and Development Agency APVV-16-0359.

Conflicts of Interest: The authors declare no conflict of interest.

References

1. Ivasishin, O.M.; Oshkaderov, S.P. Effect of rate of heating for hardening on the structure of alloys VT23 and VT6. *Met. Sci. Heat Treat.* **1982**, *24*, 459–462. [[CrossRef](#)]
2. Matokhnyuk, L.E.; Voinalovich, A.V.; Khlyapov, A.A.; Bulgakova, S.G.; Artyushina, V.P. Fatigue limit of the titanium alloy VT23 in tests with high loading frequency. *Met. Sci. Heat Treat.* **1988**, *30*, 786–789. [[CrossRef](#)]
3. Khorev, A.I. Development of structural titanium alloys for components and sections in aerospace technology. *Weld. Int.* **2010**, *24*, 790–798. [[CrossRef](#)]
4. Khorev, A.T.; Babaréko, A.A.; Krasnozhon, A.I.; Betsofen, S.Y. Effect of structure, substructure, and crystallographic texture on the mechanical properties of titanium alloys. *Met. Sci. Heat Treat.* **1982**, *24*, 463–467. [[CrossRef](#)]

5. Il'in, A.A.; Kollerov, M.Y.; Zasyupkin, V.V.; Maistrov, V.M. Volume changes occurring in ($\alpha + \beta$)-titanium alloys during polymorphic transformation. *Met. Sci. Heat Treat.* **1986**, *28*, 68–72. [[CrossRef](#)]
6. Khorev, A.I. Alloying and heat treatment of structural ($\alpha + \beta$) titanium alloys of high and superhigh strength. *Russ. Eng. Res.* **2010**, *30*, 682–688. [[CrossRef](#)]
7. Polyanskii, V.M.; Klyatskina, V.Y.; Silis, M.I. Evaluation of the brittleness of titanium alloys in terms of mechanical properties and fracture patterns. *Met. Sci. Heat Treat.* **2003**, *45*, 61–64. [[CrossRef](#)]
8. Lyasotskaya, V.S.; Khorev, A.I.; Sergeev, K.N.; Knyazeva, S.I.; Gorbunova, I.L. Improvement in the properties of alloy VT23 large semifinished products by thermal cycling treatments. *Met. Sci. Heat Treat.* **1992**, *24*, 70–73. [[CrossRef](#)]
9. Zherebtsov, S.V.; Salishchev, G.A.; Galeev, R.M. Formation of submicrocrystalline structure in titanium and its alloy under severe plastic deformation. *Defect Diffus. Forum* **2002**, *208–209*, 237–240. [[CrossRef](#)]
10. Sergeev, V.; Kalashnikov, M.P.; Neufeld, V.V. Changing of the structural-phase state and mechanical properties of VT-23 titanium alloy under surface treatment by intense flux of copper ions. *Adv. Mater. Res.* **2015**, *1085*, 284–288. [[CrossRef](#)]
11. Meshcheryakov, Y.I.; Khantuleva, T.A. Nonequilibrium processes in condensed media. Part 2. Structural instability induced by shock loading. *Phys. Mesomech.* **2016**, *19*, 69–76. [[CrossRef](#)]
12. Olemskoi, A.I. *Theory of Structure Transformations in Non-Equilibrium Condensed Matters*; Nova Science Publ. Inc.: New York, NY, USA, 1999; p. 285.
13. Mikhailov, A.S.; Ertl, G. Nonequilibrium structures in condensed systems. *Science* **1996**, *272*, 1596–1597. [[CrossRef](#)]
14. Mescheryakov, Y.I.; Divakov, A.K. Affect of shock-induced phase transformations on dynamic strength of titanium alloys. *Int. J. Impact Eng.* **2001**, *26*, 497–508. [[CrossRef](#)]
15. Mescheryakov, Y.I.; Divakov, A.K.; Zhigacheva, N.I. Shock-induced structural transitions and dynamic strength of solids. *Int. J. Solids Struct.* **2004**, *41*, 2349–2362. [[CrossRef](#)]
16. Hutsaylyuk, V.; Chausov, M.; Berezin, V.; Pylypenko, A. Strength analysis of mechanical systems at dynamic non-equilibrium processes. *Eng. Fail. Anal.* **2013**, *35*, 636–644. [[CrossRef](#)]
17. Chausov, N.G.; Voityuk, D.G.; Pilipenko, A.P.; Kuz'menko, A.M. Setup for testing materials with plotting complete stress-strain diagrams. *Strength Mater.* **2004**, *36*, 532–537. [[CrossRef](#)]
18. Chausov, N.G.; Pilipenko, A.P. Influence of dynamic overloading on fracture kinetics of metals at the final stages of deformation. *Mechanika* **2004**, *48*, 13–18.
19. Chausov, M.G.; Berezin, V.B.; Pylypenko, A.P.; Hutsaylyuk, V.B. Strain field evolution on the surface of aluminum sheet alloys exposed to specific impact with oscillation loading. *J. Strain. Anal.* **2014**, *50*, 61–62. [[CrossRef](#)]
20. Chausov, M.; Hutsaylyuk, V.; Sniezek, L.; Pylypenko, A.; Sobchak, A. Strain field evolution on the surface of stainless sheet steel 12Cr17 exposed to a specific impact with oscillation loading. In Proceedings of the 11th Int. Conf. on Intelligent Technologies in Logistics and Mechatronics Systems (ITELMS), Panevėžys, Lithuania, 28–29 April 2016.
21. Zasimchuk, E.E.; Markashova, L.I.; Tutchak, T.V.; Chausov, N.G.; Pylypenko, A.P.; Paratsa, V.N. Peculiarities of structural transformation in plastic materials under abrupt changes in loading conditions. *Phys. Mesomech.* **2009**, *12*, 175–179. [[CrossRef](#)]
22. Chausov, M.; Zasimchuk, E.; Hutsaylyuk, V.; Volyanskaya, E. Research methods of properties of dissipative structures formed while the impulse energy input into the material. *J. Ternopil National Tech. Univ.* **2011**, *2*, 92–97. (In Ukrainian)
23. Chausov, M.G.; Pylypenko, A.P.; Berezin, V.B.; Markashova, L.I.; Kushnariova, O.S.; Hutsaylyuk, V.B. Influence of impact-oscillatory loading upon the mechanical properties of the VT-22 titanium alloy sheet. *J. Mater. Eng. Perform.* **2016**, *25*, 3482–3492. [[CrossRef](#)]
24. Chausov, M.G.; Kaplunenko, V.G.; Kosinov, M.V.; Porokhnyuk, K.M. Method of the Modification of Mechanical Properties of Materials. Patent of Ukraine N 98493; Decl. 29 December 2009; Publ. 25 May 2012 (In Ukrainian).
25. Azharonok, V.V.; Lopat'ko, K.G.; Aftandilyants, E.G. Influence of acoustic and electromagnetic actions on the properties of aqueous nanoparticle dispersions used as tempering liquids for dental cement. *J. Eng. Phys. Thermophys.* **2016**, *89*, 702–713. [[CrossRef](#)]

26. Chausov, M.; Maruschak, P.; Prentkovskis, O.; Karpets, M. Risks Associated with the Use of High-Strength Titanium Alloys in Transportation Systems. In *Reliability and Statistics in Transportation and Communication, Proceedings of Lecture Notes in Networks and Systems, Riga, Latvia, 18–21 October 2017*; Kabashkin, I., Yatskiv, I., Prentkovskis, O., Eds.; Springer: New York, NY, USA, 2018; pp. 213–220.
27. Papaphilippou, C.; Pantelis, D. Laser surface alloying by injection of aluminum particles on AFNOR 45SCD6 steel. *Mater. Lett.* **1992**, *14*, 203–206. [[CrossRef](#)]
28. Kharchenko, D.; Kharchenko, V. Nano-Sized Pattern Formation in Nonequilibrium Adsorptive Systems with Interacting Adsorbate. In *Nanophysics, Nanophotonics, Surface Studies, and Applications, Springer Proceedings in Physics, Lviv, Ukraine, 26–30 2015*; Fesenko, O., Yatsenko, L., Eds.; Springer: New York, NY, USA, 2016; p. 183.
29. Kharchenko, V.O.; Kharchenko, D.O. Statistical properties of abnormal nano-sized adsorbate islands growth in a model of adsorptive multilayer system. *Surface Sci.* **2015**, *637–638*, 90–100. [[CrossRef](#)]
30. Ji, Z.; Yang, H. Microstructural design of two-phase titanium alloys by micro-scale strain distribution. *Mater. Lett.* **2016**, *184*, 157–161. [[CrossRef](#)]
31. Chausov, M.; Brezinová, J.; Pylypenko, A.; Maruschak, P.; Titova, L.; Guzanová, A. Modification of mechanical properties of high-strength titanium alloys VT23 and VT23M due to impact-oscillatory loading. *Metals* **2019**, *9*, 80. [[CrossRef](#)]



© 2019 by the authors. Licensee MDPI, Basel, Switzerland. This article is an open access article distributed under the terms and conditions of the Creative Commons Attribution (CC BY) license (<http://creativecommons.org/licenses/by/4.0/>).